

Data-based Moving Horizon Estimation under Irregularly Measured Data*

Tobias M. Wolff* Isabelle Krauss* Victor G. Lopez*
Matthias A. Müller*

* Leibniz University Hannover, Institute of Automatic Control, 30167
Hannover Germany, (e-mail: {wolff, krauss, lopez,
mueller}@irt.uni-hannover.de).

Abstract: In this work, we introduce a sample- and data-based moving horizon estimation framework for linear systems. We perform state estimation in a sample-based fashion in the sense that we assume to have only few, irregular output measurements available. This setting is encountered in applications where measuring is expensive or time-consuming. Furthermore, the state estimation framework does not rely on a standard mathematical model, but on an implicit system representation based on measured data. We prove sample-based practical robust exponential stability of the proposed estimator under mild assumptions. Furthermore, we apply the proposed scheme to estimate the states of a gastrointestinal tract absorption system.

Keywords: Data-based Estimation, Optimal control, Irregular measurements

1. INTRODUCTION

This work is centered around state estimation, which is needed for, e.g., control, monitoring and fault diagnosis. The most commonly applied state estimation methods are the Kalman filter and the Luenberger observer. Another powerful method is moving horizon estimation (MHE) - an optimization-based state estimation technique (Rawlings et al., 2017). Compared to other state estimation methods, MHE can consider system-inherent constraints directly in the estimation process.

Standard moving horizon estimation is based on the knowledge of an accurate mathematical model. Obtaining such a model can be time-consuming and difficult. Hence, in this work we represent the system dynamics by means of an implicit system representation based on the so-called fundamental lemma (Willems et al., 2005). Using a single persistently exciting trajectory of a controllable system, we can represent any finite-length behavior of that system. This result led to a large body of literature related to data-based control, such as, e.g., predictive control (Berberich et al., 2020; Coulson et al., 2019) and state feedback control (De Persis and Tesi, 2019), compare also the survey from Markovsky and Dörfler (2021). In recent years, also data-based state estimation received more attention, such as, e.g., data-based unknown input observers (Turan and Ferrari-Trecate, 2022), observers based on the duality principle of control and estimation (Adachi and Wakasa, 2021), data-based variants of the Kalman filter (Liu et al., 2024; Mishra et al., 2024), and data-based moving horizon estimation frameworks (Wolff et al., 2024a).

However, these data-based state estimation methods require online output measurements at every time instant.

This might be a restrictive assumption in many applications where measuring at each time instant is expensive, time-consuming, or even impossible. Consider, e.g., biomedical applications in which measuring some plasma hormone concentration implies to take a blood sample in a medical facility which is then analyzed in a separate laboratory. This whole process cannot be repeated too often for cost and time reasons.

In the state estimation context, few works systematically handle irregular output measurements (Krauss et al., 2025a; Mishra et al., 2024). Krauss et al. (2025a) introduce a *model-based* MHE scheme for general nonlinear systems that uses irregular output measurements (i.e., a sample-based MHE scheme). The authors exploit the concept of sample-based detectability introduced in Krauss et al. (2025b) to show robust stability of the state estimation error. In Mishra et al. (2024), a data-based state estimator for linear systems was proposed, which leverages the interpolation procedure presented in Markovsky and Dörfler (2022) to recover full-length output sequences.

In contrast to these works, here we develop a *sample- and data-based* MHE framework for linear systems (Section 3). Different from Krauss et al. (2025a), no knowledge of the mathematical model of the system is required. Furthermore, different from Mishra et al. (2024), our scheme does not perform any intermediate interpolation step and can also handle the case where no online measurements are available in a certain time window. We prove robust stability of the proposed estimator given a suitable sample-based detectability assumption (Section 4). In a simulation study on a biomedical application, we show that the performance of the sample- and data-based MHE framework can be close to the performance of a benchmark data-based MHE framework albeit using substantially less output measurements (Section 5).

* This project has received funding from the European Research Council (ERC) under the European Union's Horizon 2020 research and innovation programme (grant agreement No 948679).

2. PRELIMINARIES AND SETUP

The set of real numbers is denoted by \mathbb{R} , the set of integers in the interval $[a, b] \subset \mathbb{R}$ by $\mathbb{I}_{[a, b]}$, and the set of integers greater than or equal to $a \in \mathbb{R}$ by $\mathbb{I}_{\geq a}$. For a symmetric positive definite matrix P and a vector $x = (x_1 \dots x_n)^\top \in \mathbb{R}^n$, we write $\|x\|_P = \sqrt{x^\top Px}$. We denote the Euclidean norm by $\|x\|_2$ and the infinity norm by $\|x\|_\infty$. The maximum (minimum) eigenvalue of a symmetric matrix P is written as $\lambda_{\max}(P)$ ($\lambda_{\min}(P)$) and the maximum generalized eigenvalue of symmetric and positive definite matrices P_1 and P_2 as $\lambda_{\max}(P_1, P_2)$, i.e., the largest scalar λ satisfying $\det(P_1 - \lambda P_2) = 0$. The identity matrix of dimension n is denoted by I_n . A function $\gamma : \mathbb{R}_{\geq 0} \rightarrow \mathbb{R}_{\geq 0}$ is of class \mathcal{K} , if γ is continuous, strictly increasing, and $\gamma(0) = 0$. A stacked window of a sequence $\{x(k)\}_{k=0}^{N-1}$ from $x(i)$ up to $x(j)$ is denoted by $x_{[i,j]} = (x(i)^\top \dots x(j)^\top)^\top$. Finally, the Hankel matrix of depth L of a stacked window $x_{[0,N-1]}$ is defined by

$$H_L(x_{[0,N-1]}) = \begin{pmatrix} x(0) & x(1) & \dots & x(N-L) \\ x(1) & x(2) & \dots & x(N-L+1) \\ \vdots & \vdots & \ddots & \vdots \\ x(L-1) & x(L) & \dots & x(N-1) \end{pmatrix}.$$

Our work heavily relies on the fundamental lemma from Willems et al. (2005), which holds for linear discrete-time systems of the following form

$$x(t+1) = Ax(t) + Bu(t) \quad (1a)$$

$$y(t) = Cx(t) + Du(t) \quad (1b)$$

with states $x \in \mathbb{R}^n$, inputs $u \in \mathbb{R}^m$, and outputs $y \in \mathbb{R}^p$. To state the fundamental lemma, we require the definition of persistence of excitation (PE).

Definition 1. An input sequence $\{u(k)\}_{k=0}^{N-1}$ is persistently exciting of order L if $\text{rank}(H_L(u_{[0,N-1]})) = mL$.

The fundamental lemma in the classical state-space framework can then be formulated as follows.

Lemma 1. (Berberich and Allgöwer (2020)) Suppose $u_{[0,N-1]}$, $y_{[0,N-1]}$ is a trajectory of a controllable LTI system (1), where $u_{[0,N-1]}$ is persistently exciting of order $L+n$. Then, $\bar{u}_{[0,L-1]}$, $\bar{y}_{[0,L-1]}$ is a trajectory of linear system (1) if and only if there exists $\alpha \in \mathbb{R}^{N-L+1}$ such that

$$\begin{bmatrix} H_L(u_{[0,N-1]}) \\ H_L(y_{[0,N-1]}) \end{bmatrix} \alpha = \begin{bmatrix} \bar{u}_{[0,L-1]} \\ \bar{y}_{[0,L-1]} \end{bmatrix}. \quad (2)$$

The lemma states that we can represent *any* finite-length trajectory of a controllable system as linear combinations of windows of one single PE trajectory.

Remark 1. In addition to Lemma 1, we note that the following also holds (Berberich and Allgöwer, 2020, Eq. (5))

$$\bar{x}_{[0,L-1]} = \sum_{i=0}^{N-L} \alpha_i x_{[i,L-1+i]}, \quad (3)$$

where $\bar{x}_{[0,L-1]}$ and $x_{[0,N-1]}$ are state trajectories of system (1) that correspond to the trajectories $\bar{u}_{[0,L-1]}$, $\bar{y}_{[0,L-1]}$ and $u_{[0,N-1]}$, $y_{[0,N-1]}$ of (1), respectively, and α_i for $i = 0, \dots, N-L$ correspond to the individual elements of the vector α in (2). This result is important in the

context of data-based state estimation as will become clear in Section 3.

Finally, Willems et al. (2005) also prove the following lemma.

Lemma 2. Suppose $x_{[0,N-1]}$, $u_{[0,N-1]}$ is an input/state trajectory of the controllable LTI system (1) where $u_{[0,N-1]}$ is persistently exciting of order $L+n$, then the matrix

$$\begin{bmatrix} H_1(x_{[0,N-L]}) \\ H_L(u_{[0,N-1]}) \end{bmatrix} \quad (4)$$

has full row rank.

In this work, we consider two phases. First, an *offline phase*, in which we have N noisy measurements of the outputs and states at every time instant available, i.e.,

$$\tilde{x}^d(t) = x^d(t) + \varepsilon_x^d(t), \quad (5)$$

$$\tilde{y}^d(t) = y^d(t) + \varepsilon_y^d(t), \quad (6)$$

where the noise-free state and output measurements are denoted by x^d and y^d , respectively. The offline state and output measurement noise are denoted by ε_x^d and ε_y^d , respectively, and we assume that $\|\varepsilon_x^d(t)\|_\infty \leq \bar{\varepsilon}_x^d$ and $\|\varepsilon_y^d(t)\|_\infty \leq \bar{\varepsilon}_y^d$. Additionally, we define

$$\bar{\varepsilon}^d = \max\{\bar{\varepsilon}_x^d, \bar{\varepsilon}_y^d\}. \quad (7)$$

The assumption of having regular state measurements available in an offline phase is standard in the data-based state estimation literature (Turan and Ferrari-Trecate, 2022; Liu et al., 2024; Mishra et al., 2024; Wolff et al., 2024a) and is needed to estimate system states in a physically meaningful realization. This setting is also fulfilled in various applications, where in a laboratory setting during the offline phase, one can equip the system with additional sensors that might be too expensive or impossible to employ during later runtime of the system (i.e., during the online phase). Having state measurements in an offline phase is crucial for the results of our work, since, as will become clear in the next section, the online state estimate will result from linear combinations of the offline state measurements. This guarantees that the online state estimates are in a physically meaningful realization. Note that without the offline measured state trajectory, the realizations of the estimated states would be unknown, since different state trajectories can explain the given input/output data as it is well known, e.g., from the context of subspace identification (Van Overschee, 1997).

In the *online phase*, we only have noisy measurements of the outputs, i.e.,

$$y(t) = Cx(t) + Du(t) + v(t) \quad (8)$$

with $v(t) \in \mathbb{V} \subset \mathbb{R}^p$ but *not* of the states available. Additionally, we allow for only *few and irregular* output measurements, which is encountered in various applications where measuring is time-consuming and/or expensive.

3. SAMPLE- AND DATA-BASED MHE FRAMEWORK

Before explaining the sample- and data-based MHE framework in detail, we first need to introduce some notation. Let $\Omega = \{t_i\}_{i=1}^\infty$ with $0 \leq t_i < t_{i+1}$ be the *infinite* set of time instances at which output measurements will be

taken during the execution of the state estimation scheme. Note that this set is used for analysis only and does not need to be fixed before the application of the estimator. Furthermore, we require a reduced Hankel matrix of the output measurements that is composed of the block rows that correspond to online measurement time instances, i.e., we introduce $H_{L_t}^{\tilde{\Omega}_t}(\tilde{y}_{[0,N-2]}^d)$, with $L_t := \min\{t, L\}$, which is a submatrix of $H_{L_t}(\tilde{y}_{[0,N-2]}^d)$. To specify the row indices of $H_{L_t}^{\tilde{\Omega}_t}$, it will be useful to define the set of “measurement block row indices” $\tilde{\Omega}_t := \{j \in \mathbb{N} | j = i - (t - L_t) + 1, i \in \Omega \cap [t - L_t, t - 1]\}$. Then, $H_{L_t}^{\tilde{\Omega}_t}$ is formed by the block rows of H_{L_t} corresponding to the indices in $\tilde{\Omega}_t$. By $\bar{x}_{[-L,0]}(t) := (\bar{x}(t - L|t)^\top \dots \bar{x}(t|t)^\top)^\top$, we denote the estimated state sequence from time $t - L_t$ up to time t , estimated at time t (and we use a similar notation for the slacks σ^x and σ^y , the role of which is explained below). The measured input sequence from time $t - L_t$ up to time $t - 1$ is denoted by $u_{[t-L_t,t-1]}$. By $\tilde{y}_{[t-L_t,t-1]\cap\Omega}$, we denote the vectors whose entries are the noisy output measurements that are in the current horizon from $t - L_t$ up to $t - 1$. Finally, we write $\sigma_{[-L_t,-1]\cap\Omega}^y(t)$ to denote¹ the estimated measurement noise at the online measurement time instances.

We are now ready to introduce the sample- and data-based MHE framework, which is based on the formulation proposed in our previous work (Wolff et al., 2024a) and extended here to the case of irregular measurements. At each time t , given a horizon length L , and input/output measurements $u_{[t-L_t,t-1]}$, $\tilde{y}_{[t-L_t,t-1]\cap\Omega}$, solve

$$\begin{aligned} & \text{minimize}_{\bar{x}_{[-L_t,0]}(t), \alpha(t), \sigma_{[-L_t,-1]\cap\Omega}^y(t), \sigma_{[-L_t,0]}^x(t)} \\ & J(\bar{x}(t - L_t|t), \sigma_{[-L_t,-1]\cap\Omega}^y(t), \sigma_{[-L_t,0]}^x(t), \alpha(t)) \end{aligned} \quad (9a)$$

$$\begin{aligned} \text{s. t. } & \begin{bmatrix} H_{L_t}(u_{[0,N-2]}^d) \\ H_{L_t}^{\tilde{\Omega}_t}(\tilde{y}_{[0,N-2]}^d) \\ H_{L_t+1}(\tilde{x}_{[0,N-1]}^d) \end{bmatrix} \alpha(t) \\ & = \begin{bmatrix} u_{[t-L_t,t-1]} \\ \tilde{y}_{[t-L_t,t-1]\cap\Omega} - \sigma_{[-L_t,-1]\cap\Omega}^y(t) \\ \bar{x}_{[-L_t,0]}(t) + \sigma_{[-L_t,0]}^x(t) \end{bmatrix} \end{aligned} \quad (9b)$$

$$\bar{x}_{[-L_t,0]}(t) \in \mathbb{X} \quad (9c)$$

with

$$\begin{aligned} & J(\bar{x}(t - L_t|t), \sigma_{[-L_t,-1]\cap\Omega}^y(t), \sigma_{[-L_t,0]}^x(t), \alpha(t)) \\ & := \Gamma(\bar{x}(t - L_t|t)) + \sum_{k \in \mathbb{I}_{[t-L_t,t-1]\cap\Omega}} l_k(\sigma^y(k|t)) \\ & + c_{\sigma^x} \|\sigma_{[-L_t,0]}^x(t)\|^2 + c_\alpha ((\bar{\varepsilon}_x^d)^2 + (\bar{\varepsilon}_y^d)^2) \|\alpha(t)\|^2. \end{aligned} \quad (9d)$$

In the cost function (9d), we consider a prior weighting defined as follows

$$\Gamma(\bar{x}(t - L_t|t)) := 2 \|\bar{x}(t - L_t|t) - \hat{x}(t - L_t)\|_{P_2}^2 \eta^{L_t}, \quad (10)$$

with a positive definite weighting matrix P_2 , the state estimate at time $t - L_t$, i.e., $\hat{x}(t - L_t)$, and a discount factor $\eta \in [0, 1)$, which will be crucial to prove robust stability as shown in Section 4. This prior weighting penalizes the deviation from the initial element of the estimated state

¹ With a slight abuse of notation, the subindex $[-L_t, -1] \cap \Omega$ here refers to the time indices in $[t - L_t, t - 1] \cap \Omega$.

sequence to the state estimate at time $t - L_t$. This type of prior weighting is called *filtering* prior in the MHE literature and has beneficial theoretical properties (Allan and Rawlings, 2019). In the second term of (9d), we penalize the estimated measurement noise σ^y at the online measurement time instances, where

$$l_k(\sigma^y(k|t)) := \|\sigma^y(k|t)\|_R^2 \eta^{t-k-1} \quad (11)$$

with a positive semi-definite R . The third and fourth term correspond to regularization terms. The term related to σ^x brings the estimated state sequence closer to the span of the offline state measurements. The term related to α limits the amplification of the noise affecting the offline state and output measurements measurement, compare also the discussion in Wolff et al. (2024a).

In the constraints (9b), we consider the span of the offline measured input/state/output trajectory. Note that the noisy online output measurements \tilde{y} might not necessarily be in the span of the noisy offline measurements. This is why we need to consider the estimated measurement noise σ^y on the right-hand side of the constraints (9b).

Furthermore, the offline measured state trajectory is also noisy, which requires the introduction of the slack σ^x in the last row of the constraints (9b). Otherwise, we cannot guarantee that the estimated state trajectory satisfies the state constraints (9c). Here, \mathbb{X} in (9c) is some known constraint set that contains all possible system states and typically corresponds to system-inherent constraints, such as nonnegativity constraints of chemical concentrations.

The solutions to the optimization problem (9) are denoted by $\hat{x}_{[-L_t,0]}(t)$, $\hat{\alpha}(t)$, $\hat{\sigma}_{[-L_t,-1]\cap\Omega}^y(t)$, and $\hat{\sigma}_{[-L_t,0]}^x(t)$. The state estimate at time t is set to the last element of the estimated sequence, i.e., $\hat{x}(t) := \hat{x}(t|t)$.

4. ROBUST STABILITY GUARANTEES

In this section, we develop robust stability guarantees of the sample- and data-based MHE scheme. Before showing the main theorem, we start by introducing some assumptions and definitions. We are interested in showing robust stability according to the following definition.

Definition 2. Consider system (1) subject to disturbances $v \in \mathbb{V}$ in the online phase, compare (8), and ε_x , ε_y in the offline phase, compare (5) - (7), respectively. A state estimator is sample-based practically robustly exponentially stable (pRES) if there exist a function $\gamma \in \mathcal{K}$, constants $c_1, c_2 \geq 0$, and $\lambda_1, \lambda_2 \in [0, 1)$ such that for all $x(0)$, $\hat{x}(0) \in \mathbb{X}$, and all $v \in \mathbb{V}$ the following is satisfied for all $t \in \mathbb{I}_{\geq 0}$:

$$\begin{aligned} & \|x(t) - \hat{x}(t)\| \leq c_1 \|x(0) - \hat{x}(0)\| \lambda_1^t \\ & + \sum_{\tau \in \mathbb{I}_{[0,t-1]\cap\Omega}} c_2 \|v(t - \tau)\| \lambda_2^\tau + \gamma(\bar{\varepsilon}^d). \end{aligned} \quad (12)$$

In the employed detectability notion (see Definition 4 below), we rely on a set K defined as follows.

Definition 3. (Krauss et al., 2025b, Def. 4) Consider an infinitely long sequence $\Delta = \{\delta_1, \delta_2, \dots\}$ with $\delta_i \in \mathbb{I}_{\geq 0}$, $i \in \mathbb{I}_{>0}$ and $\max_i \delta_i =: \delta_{\max} < \infty$. The set $K_i = \{t_1^i, t_2^i, \dots\}$ refers to an infinite set of time instances defined as

$$t_1^i = \delta_i, \quad t_2^i = t_1^i + \delta_{i+1}, \quad \dots, \quad t_j^i = t_{j-1}^i + \delta_{i+j-1}, \quad \dots$$

The set K then refers to a set of sets containing all K_i , $i \in \mathbb{I}_{\geq 0}$.

The set Δ defines a pattern for taking samples at certain time instances. The set K_i corresponds to one such possible sampling scheme that starts at δ_i , and K is a set of sets containing all the possible sampling schemes K_i compatible with Δ . This definition is useful to analyze detectability uniformly in time. We refer the interested reader to Krauss et al. (2025b) for a more detailed discussion regarding Definition 3.

Next, we define our crucial detectability notion, namely sample-based uniform exponential incremental output-to-state stability (i-OSS). In this definition we use $h(x, u) := Cx + Du$.

Definition 4. System (1) is sample-based uniformly exponentially i-OSS with respect to the sampling set K if there exist $P_1, P_2 \succ 0$, $R \succeq 0$ and $\eta \in [0, 1)$ such that for any pair of initial conditions $\tilde{x}(0), \tilde{x}'(0) \in \mathbb{X}$ and for all input sequences $\{u(k)\}_{k=0}^{\infty}$ it holds for all $t \geq 0$ and any $K_i \in K$ that

$$\begin{aligned} \|\tilde{x}(t) - \tilde{x}'(t)\|_{P_1}^2 &\leq \|\tilde{x}(0) - \tilde{x}'(0)\|_{P_2}^2 \eta^t \\ &+ \sum_{j \in \mathbb{I}_{[0, t-1]} \cap K_i} \eta^{t-j-1} \|h(\tilde{x}(j), u(j)) - h(\tilde{x}'(j), u(j))\|_R^2. \end{aligned} \quad (13)$$

This notion corresponds to a sample-based and exponential version of incremental input/output-to-state stability (i-IOSS), which has been used frequently in the MHE literature to prove stability of various MHE schemes (Knüfer and Müller, 2018; Allan et al., 2021; Hu, 2023). In fact, i-IOSS is necessary and sufficient for the existence of a robustly stable state estimator (Knüfer and Müller, 2020; Allan and Rawlings, 2021; Knüfer and Müller, 2023). Here, we consider a sample-based and exponential variant of the standard i-IOSS notion and do not consider inputs (i.e., process noise in (1a)), since the fundamental lemma is defined for systems without process noise, compare the discussion in (Wolff et al., 2024a, Rmk. 4) for possible extensions to the case of additional process noise. Here, the “uniformity” notion is employed since the right-hand side in Definition 4 holds uniformly for all control input sequences.

To prove robust stability, we need the following detectability assumption.

Assumption 1. Consider a set K as in Definition 3. System (1) is sample-based exponential i-OSS according to Definition 4 for this K . Moreover, for the actual set of measurement time instances Ω , it holds that $\Omega \in K$.

Conditions for Assumption 1 to hold for linear systems (1) are investigated in Krauss et al. (2025a).

Furthermore, we need to ensure that we collect sufficiently rich data in the offline phase as stated in the following assumption.

Assumption 2. The considered system (1) is controllable and the offline input $\{u^d(k)\}_{k=0}^{N-1}$ applied to the system is persistently exciting of order $L + n + 1$.

Next, we require that the states and inputs evolve in compact sets.

Assumption 3. The states x and control inputs u of system (1) evolve in compact sets \mathbb{U} and \mathbb{X} , i.e., $u(t) \in \mathbb{U}$ and $x(t) \in \mathbb{X}$ for all $t \in \mathbb{I}_{\geq 0}$, respectively.

If necessary, one can apply a pre-stabilizing controller to guarantee that the states of the system do not grow unboundedly. Furthermore, in most cases, the control inputs have certain actuator limits, which means that one can easily find a corresponding set \mathbb{U} .

We are now ready to state the main theorem of this work. In this theorem, we give sufficient conditions for the existence of a minimal horizon length L_{\min} such that the proposed estimator is sample-based pRES.

Theorem 1. Consider that noisy offline data as specified in (5) and (6) and noisy online data as defined in (8) are available to the sample- and data-based MHE framework (9). Let Assumptions 1 - 3 hold and the horizon length $L \in \mathbb{I}_{\geq \delta_{\max}}$ be chosen such that $16\lambda_{\max}(P_2, P_1)^2\eta^L < 1$ is satisfied. Moreover, let c_{α} and c_{σ^x} in (9d) be such that

$$c_{\alpha} \geq \max \left\{ \left(2\lambda_{\max}(P_2) + \frac{\lambda_{\max}(P_1)}{\lambda_{\max}(P_2, P_1)} \right) nN, \frac{2\eta - \eta^L}{1 - \eta} pN \frac{\lambda_{\max}(R)}{\lambda_{\max}(P_2, P_1)} \right\} \quad (14)$$

$$c_{\sigma^x} \geq \max \left\{ 2\lambda_{\max}(P_2), \frac{\lambda_{\max}(P_1)}{\lambda_{\max}(P_2, P_1)} \right\}. \quad (15)$$

Then, there exist $\tilde{\rho} \in [0, 1)$ and $\tilde{\gamma} \in \mathcal{K}$ such that the state estimation error satisfies the following bound for all times $t \in \mathbb{I}_{\geq 0}$

$$\begin{aligned} \|x(t) - \hat{x}(t)\|_{P_1} &\leq 4\tilde{\rho}^t \sqrt{\lambda_{\max}(P_2, P_1)} \|x(0) - \hat{x}(0)\|_{P_2} \\ &+ \sqrt{8 + 4\lambda_{\max}(P_2, P_1)} \sum_{k \in \mathbb{I}_{[0, t-1]} \cap \Omega} \|v(k)\|_R \tilde{\rho}^{t-k-1} + \tilde{\gamma}(\tilde{\varepsilon}^d). \end{aligned} \quad (16)$$

Hence, the sample- and data-based MHE scheme is sample-based pRES according to Definition 2.

The proof of the theorem is given in the Appendix. The proof uses ideas from model- and sample-based (Krauss et al., 2025a), and data-based MHE robust stability proofs (Wolff et al., 2024a).

Remark 2. In the proof of Theorem 1 (in particular in (A.14) and (A.16)), it becomes clear that the function $\tilde{\gamma}$ in the error bound (16) increases as the horizon length L increases. This drawback is caused by our proof strategy, where we find bounds for the regularization terms in the cost function that depend on L . In practice, it is known that increasing the horizon length does not worsen the estimator performance, and modifying our current proof to reflect this fact is a subject for future work.

Remark 3. If one considers noise-free offline state and output measurements which might be the case if very accurate sensors are used, we can omit the slack σ^x , since the estimated states will always satisfy the constraints. We also do not need to regularize α in the cost function. The robust stability proof can be modified accordingly by considering these changes and $\tilde{\varepsilon}_x^d = \tilde{\varepsilon}_y^d = 0$. A standard data-based MHE framework with such a setting is considered in Wolff et al. (2022). For this setting, the

resulting function $\tilde{\gamma}$ in (16) is then *independent* of the horizon length L .

Remark 4. The sample- and data-based MHE framework presented here considers potentially infrequent output measurements in the online phase, but full measurements in the offline phase. In fact, it is possible to consider also irregular offline measurements by leveraging the results presented in Alsalti et al. (2025). As is shown there, under certain conditions it is possible to construct an implicit data-based system representation only based on trajectories with missing samples. Hence, we could also use this implicit system representation instead of the fundamental lemma to cover this case.

5. APPLICATION TO GASTROINTESTINAL TRACT ABSORPTION

In this section, we apply the sample- and data-based MHE scheme to a biomedical example. In particular, we consider the gastrointestinal tract absorption of an oral medication intake from Mak and DiStefano III (1978) with adapted parameters to better visualize the results. As medication, we consider *levothyroxine* (L-T₄) that is needed in case of hypothyroidism (which is a consequence of the autoimmune disease called Hashimoto's thyroiditis) to replace the missing endogenously produced thyroxine. We here consider the following dynamics

$$\dot{x}_1(t) = -k_1 x_1(t) + u(t) \quad (17a)$$

$$\dot{x}_2(t) = k_1 x_1(t) - (k_2 + k_3) x_2(t) \quad (17b)$$

$$y(t) = k_3 x_2(t) \quad (17c)$$

with $k_1 = 1.3$, $k_2 = 0.15$, and $k_3 = 0.15$. The first state corresponds to the undissolved medication in the gut and the second state to the dissolved medication in the gut. The control input u corresponds to the medication intake. The output measurements are the concentrations of L-T₄ in the blood.

We discretize the dynamics exactly with a sampling time of $\delta = 15$ min and simulate an offline input/state/output sequence of length $N = 67$. We consider noisy measurements as detailed in (5) and (6) with ε_x^d and ε_y^d , respectively, sampled from a truncated normal distribution with zero mean and variance $\sigma_{\varepsilon_x^d}^2 = \sigma_{\varepsilon_y^d}^2 = 0.01$. We then choose $\eta = 0.98$, $R = 10^8$ (a large value is necessary to give enough weight to the few measurements that are in the current horizon), $P_2 = I_n$, $c_\alpha = 2 \cdot 10^7$ and $c_{\sigma_x} = 2 \cdot 10^7$, and construct the Hankel matrices as required in (9).

In the online phase, we consider some measurement noise sampled from a truncated normal distribution with zero mean and variance $\sigma_v^2 = 0.03$. The horizon length is chosen as $L = 32$. The prior estimate is set to $\hat{x}(0) = (0 \ 0)^\top$ and the true initial condition to $x(0) = (0.3 \ 0.3)^\top$. We simulate the concentrations throughout one day, i.e., $N_{\text{sim}} = 96$.

We first simulate the case, where a complete output sequence (i.e., no missing measurements) is available to the state estimation scheme. This serves as benchmark for the following simulations, where we assume to have only *few and irregular* measurements available. The simulation results are shown in the top plot of Figure 1. As expected, we observe a very good performance of the proposed MHE framework in the benchmark case.

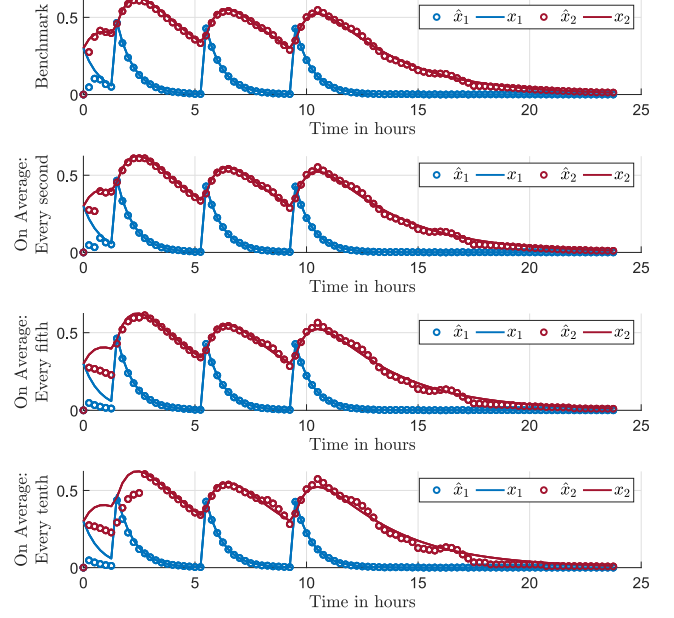


Fig. 1. Simulation results of system (17) for four different settings.

In the first plot, we consider that all output measurements are available to the state estimation scheme (benchmark case). In the following three plots, we consider that the state estimation scheme has only 48, 19, and 9 random measurement available.

	MSE
Benchmark	$2.40 \cdot 10^{-3}$
48 measurements (on average every second)	$5.90 \cdot 10^{-3}$
19 measurements (on average every fifth)	$1.41 \cdot 10^{-2}$
9 measurements (on average every tenth)	$1.43 \cdot 10^{-2}$

Table 1. Performance comparison for system (17).

Next, we perform three different simulations considering irregular measurements. In the first simulation, we assume that 48 random measurements (i.e., on average every second sample) are available to the estimation scheme. In the second and third simulation, we assume that 19 random measurements (i.e., on average every fifth sample) and 9 random measurements (i.e., on average every tenth sample), respectively, are available to the estimation scheme. The simulation results of all of these simulations are displayed in Figure 1.

In addition to the plots, we compute the mean squared error (MSE) defined as

$$\text{MSE} = \frac{1}{N_{\text{sim}}} \sum_{k=1}^{N_{\text{sim}}} \|x(k) - \hat{x}(k)\|^2 \quad (18)$$

in all simulations and show the results in Table 1.

From Table 1 and Figure 1, we obtain the expected result that having all output measurements available results in the best MSE, and that the performance degrades as fewer measurements are taken. In the remaining cases, we first note that the proposed estimator overall performs very well. Second, we conclude that the performance declines only slightly as irregular measurements are taken compared to the benchmark performance. Third, the difference

in the performance when considering on average every fifth and every tenth measurement is small. This is due to the fact that the MSE is dominated by the first samples in which we have a considerably larger estimation error compared to the steady state.

6. CONCLUSION

In this work, we introduced a sample- and data-based MHE framework, which exploits the fundamental lemma to obtain a purely data-based system representation. Furthermore, the estimation scheme is designed such that it can handle few and irregular measurements. Finally, we developed robust stability guarantees for the framework. In a biomedical example, we showed that the proposed estimator performs very well, even in the case where few measurements are considered.

Our work focuses on the linear case, although MHE has been proven to be very powerful for nonlinear systems. Hence, an extension of our work to nonlinear systems would be interesting.

REFERENCES

Adachi, R. and Wakasa, Y. (2021). Dual system representation and prediction method for data-driven estimation. In *2021 60th Annual Conference of the Society of Instrument and Control Engineers of Japan (SICE)*, 1245–1250. IEEE.

Allan, D.A., Rawlings, J., and Teel, A.R. (2021). Nonlinear detectability and incremental input/output-to-state stability. *SIAM Journal on Control and Optimization*, 59(4), 3017–3039.

Allan, D.A. and Rawlings, J.B. (2019). Moving horizon estimation. In S.V. Raković and W.S. Levine (eds.), *Handbook of Model Predictive Control*, 99–124. Springer International Publishing, Cham.

Allan, D.A. and Rawlings, J.B. (2021). Robust stability of full information estimation. *SIAM Journal on Control and Optimization*, 59(5), 3472–3497.

Alsalti, M., Markovsky, I., Lopez, V.G., and Müller, M.A. (2025). Data-based system representations from irregularly measured data. *IEEE Transactions on Automatic Control*, 70(1), 143–158.

Berberich, J. and Allgöwer, F. (2020). A trajectory-based framework for data-driven system analysis and control. In *2020 European Control Conference (ECC)*, 1365–1370. IEEE.

Berberich, J., Köhler, J., Müller, M.A., and Allgöwer, F. (2020). Data-driven model predictive control with stability and robustness guarantees. *IEEE Transactions on Automatic Control*, 66(4), 1702–1717.

Coulson, J., Lygeros, J., and Dörfler, F. (2019). Data-enabled predictive control: In the shallows of the DeePC. In *2019 18th European Control Conference (ECC)*, 307–312. IEEE.

De Persis, C. and Tesi, P. (2019). Formulas for data-driven control: Stabilization, optimality, and robustness. *IEEE Transactions on Automatic Control*, 65(3), 909–924.

Hu, W. (2023). Generic stability implication from full information estimation to moving-horizon estimation. *IEEE Transactions on Automatic Control*, 69(2), 1164–1170.

Knüfer, S. and Müller, M.A. (2020). Time-discounted incremental input/output-to-state stability. In *2020 59th IEEE Conference on Decision and Control (CDC)*, 5394–5400. IEEE.

Knüfer, S. and Müller, M.A. (2023). Nonlinear full information and moving horizon estimation: Robust global asymptotic stability. *Automatica*, 150, 110603.

Knüfer, S. and Müller, M.A. (2018). Robust global exponential stability for moving horizon estimation. In *2018 IEEE Conference on Decision and Control (CDC)*, 3477–3482.

Krauss, I., Lopez, V.G., and Müller, M.A. (2025a). Sample-based moving horizon estimation. *arXiv: 2510.24191*.

Krauss, I., Lopez, V.G., and Müller, M.A. (2025b). Sample-based nonlinear detectability for discrete-time systems. *IEEE Transactions on Automatic Control*, 70(4), 2422–2434.

Liu, W., Wang, G., Sun, J., Bullo, F., and Chen, J. (2024). Learning robust data-based LQG controllers from noisy data. *IEEE Transactions on Automatic Control*, 69(12).

Mak, P.H. and DiStefano III, J.J. (1978). Optimal control policies for the prescription of thyroid hormones. *Mathematical Biosciences*, 42(3-4), 159–186.

Markovsky, I. and Dörfler, F. (2021). Behavioral systems theory in data-driven analysis, signal processing, and control. *Annual Reviews in Control*, 52, 42–64.

Markovsky, I. and Dörfler, F. (2022). Data-driven dynamic interpolation and approximation. *Automatica*, 135, 110008.

Mishra, V.K., Hirmath, S.A., and Bajcinca, N. (2024). Data-driven state estimation for linear systems. In *2024 European Control Conference (ECC)*, 906–913. IEEE.

Rawlings, J.B., Mayne, D.Q., and Diehl, M. (2017). *Model predictive control: theory, computation, and design*, volume 2. Nob Hill Publishing Madison, WI.

Schiller, J.D., Muntwiler, S., Köhler, J., Zeilinger, M.N., and Müller, M.A. (2023). A Lyapunov function for robust stability of moving horizon estimation. *IEEE Transactions on Automatic Control*, 68(12), 7466–7481.

Turan, M.S. and Ferrari-Trecate, G. (2022). Data-driven unknown-input observers and state estimation. *IEEE Control Systems Letters*, 6, 1424–1429.

Van Overschee, P. (1997). Subspace identification: Theory, implementation, application.

Willems, J.C., Rapisarda, P., Markovsky, I., and De Moor, B.L. (2005). A note on persistency of excitation. *Systems & Control Letters*, 54(4), 325–329.

Wolff, T.M., Lopez, V.G., and Müller, M.A. (2022). Data-based moving horizon estimation for linear discrete-time systems. In *2022 European Control Conference (ECC)*, 1778–1783.

Wolff, T.M., Lopez, V.G., and Müller, M.A. (2024a). Robust data-driven moving horizon estimation for linear discrete-time systems. *IEEE Transactions on Automatic Control*, 69(8), 5598–5604.

Wolff, T.M., Lopez, V.G., and Müller, M.A. (2024b). Robust data-driven moving horizon estimation for linear discrete-time systems (extended version). *arXiv: 2210.09017*.

Appendix A. PROOF OF THEOREM 1

For a better readability, the proof is divided in three parts. The first part is the construction of a candidate solution for the optimization problem and follows identically from (Wolff et al., 2024b, Eq. (22) - (27)). In the second part, we exploit this candidate trajectory together with the optimal solution in the sample-based exponential i-OSS property. In the last part, we combine the sample-based exponential i-OSS property with solutions of the MHE optimization problem to finally prove robust stability.

Proof: Part I: Construction of a candidate trajectory.

The candidate trajectory for the optimization problem (9) to be used in the remainder of this proof is described in (Wolff et al., 2024b, Eqs. (22) - (27)) and not shown here for space reasons. Note that we here consider the trajectory from time $t - L_t$ up to time t instead of time 0 up to time t , as shown in Wolff et al. (2024b).

Part II: Exploitation of the exponential i-OSS property.

Please note that the first steps of this second part have already been developed in (Wolff et al., 2024b, Thm. 2).

In the sample-based exponential i-OSS property, we consider the real unknown state trajectory parameterized by means of the candidate α , compare (Wolff et al., 2024b, Eq. (22)). This real state trajectory starts at $\tilde{x}(t - L_t) = x(t - L_t)$. Its value at time t corresponds to $\tilde{x}(t) = x(t)$. Furthermore, we consider a state trajectory based on the estimated state sequence. For this, we consider a sequence starting at

$$\begin{aligned}\tilde{x}'(t - L_t) &= \\ \hat{x}(t - L_t | t) - H_1(\varepsilon_{x,[0,N-L_t]}^d) \hat{\alpha}(t) + \hat{\sigma}^x(t - L_t | t) \\ &= H_1(x_{[0,N-L_t]}^d) \hat{\alpha}(t),\end{aligned}\quad (\text{A.1})$$

which can be deduced from the last row of (9b). After L_t time instances, the state value becomes

$$\begin{aligned}\tilde{x}'(t) &= \hat{x}(t | t) - H_1(\varepsilon_{x,[L_t-1,N-1]}^d) \hat{\alpha}(t) + \hat{\sigma}^x(t | t) \\ &= H_1(x_{[L_t-1,N-1]}^d) \hat{\alpha}(t).\end{aligned}\quad (\text{A.2})$$

Therefore,

$$\begin{aligned}\|\tilde{x}(t) - \tilde{x}'(t)\|_{P_1} &= \\ \|\hat{x}(t) - \hat{x}(t) + H_1(\varepsilon_{x,[L_t-1,N-1]}^d) \hat{\alpha}(t) - \hat{\sigma}^x(t | t)\|_{P_1} &= \\ \|\hat{x}(t) - \tilde{x}'(t)\|_{P_1} &.\end{aligned}$$

Note that $\|a\| - \|b\| \leq \|a - b\|$ for any vectors a and b , which implies

$$\begin{aligned}\|\hat{x}(t) - \hat{x}(t)\|_{P_1} - \|H_1(\varepsilon_{x,[L_t-1,N-1]}^d) \hat{\alpha}(t) + \hat{\sigma}^x(t | t)\|_{P_1} \\ \leq \|\hat{x}(t) - \hat{x}(t) + H_1(\varepsilon_{x,[L_t-1,N-1]}^d) \hat{\alpha}(t) - \hat{\sigma}^x(t | t)\|_{P_1} \\ = \|\tilde{x}(t) - \tilde{x}'(t)\|_{P_1}.\end{aligned}$$

Reformulating the above inequality and considering the squared version yields

$$\begin{aligned}\|\hat{x}(t) - \hat{x}(t)\|_{P_1}^2 &\leq 2\|\tilde{x}(t) - \tilde{x}'(t)\|_{P_1}^2 \\ &\quad + 2\|H_1(\varepsilon_{x,[L_t-1,N-1]}^d) \hat{\alpha}(t) + \hat{\sigma}^x(t | t)\|_{P_1}^2,\end{aligned}$$

where we used the fact that $\|a + b\|_{P_1}^2 \leq 2\|a\|_{P_1}^2 + 2\|b\|_{P_1}^2$ for any vectors a, b .

In the following, we use a similar procedure as in Krauss et al. (2025a). We introduce $\psi_\tau := \min\{i | i \in [\tau, \infty) \cap \Omega\} - \tau$. Note that there is a measurement at time $t - L_t + \psi_{t-L_t}$. Consequently, the following measurements in the interval $[t - L_t + \psi_{t-L_t}, t - 1]$ correspond to the pattern given in Definition 3 using a contiguous subsequence of Δ . Then, we can replace the difference $\|\tilde{x}(t) - \tilde{x}'(t)\|_{P_1}^2$ by means of the sample-based exponential i-OSS condition (recall Definition 4, Assumption 1, and (A.1)) and obtain

$$\begin{aligned}\|\hat{x}(t) - \hat{x}(t)\|_{P_1}^2 &\leq 2\|\tilde{x}(t - L_t + \psi_{t-L_t}) - \tilde{x}'(t - L_t + \psi_{t-L_t})\|_{P_2}^2 \eta^{L_t - \psi_{t-L_t}} \\ &\quad + 2 \sum_{k \in \mathbb{I}_{[t-L_t+\psi_{t-L_t},t-1]} \cap \Omega} \eta^{t-k-1} \|h(\tilde{x}(k), u(k)) \\ &\quad \quad - h(\tilde{x}'(k), u(k))\|_R^2 \\ &\quad + 2\|H_1(\varepsilon_{x,[L_t-1,N-1]}^d) \hat{\alpha}(t) + \hat{\sigma}^x(t | t)\|_{P_1}^2.\end{aligned}\quad (\text{A.3})$$

Since $\psi_{t-L_t} \leq \delta_{\max}$, and since there are no measurements in the interval $[t - L_t, t - L_t + \psi_{t-L_t} - 1]$, it follows from Assumption 1 and the properties of the generalized eigenvalues that

$$\begin{aligned}\|\tilde{x}(t - L_t + \psi_{t-L_t}) - \tilde{x}'(t - L_t + \psi_{t-L_t})\|_{P_2}^2 &\leq \lambda_{\max}(P_2, P_1) \|\tilde{x}(t - L_t + \psi_{t-L_t}) \\ &\quad - \tilde{x}'(t - L_t + \psi_{t-L_t})\|_{P_2}^2 \\ &\leq \lambda_{\max}(P_2, P_1) \eta^{\psi_{t-L_t}} \|\tilde{x}(t - L_t) - \tilde{x}'(t - L_t)\|_{P_2}^2.\end{aligned}\quad (\text{A.4})$$

Substituting (A.4) in (A.3) results in

$$\begin{aligned}\|x(t) - \hat{x}(t)\|_{P_1}^2 &\leq 2\lambda_{\max}(P_2, P_1) \eta^{L_t} \|\tilde{x}(t - L_t) - \tilde{x}'(t - L_t)\|_{P_2}^2 \\ &\quad + 2 \sum_{k \in \mathbb{I}_{[t-L_t,t-1]} \cap \Omega} \eta^{t-k-1} \|h(\tilde{x}(k), u(k)) \\ &\quad \quad - h(\tilde{x}'(k), u(k))\|_R^2 \\ &\quad + 2\|H_1(\varepsilon_{x,[L_t-1,N-1]}^d) \hat{\alpha}(t) + \hat{\sigma}^x(t | t)\|_{P_1}^2.\end{aligned}$$

We replace \tilde{x} and \tilde{x}' in the first term as explained at the beginning of Part II above and obtain

$$\begin{aligned}\|x(t) - \hat{x}(t)\|_{P_1}^2 &\leq 2\lambda_{\max}(P_2, P_1) \eta^{L_t} \|x(t - L_t) - \hat{x}(t - L_t | t)\|_{P_2}^2 \\ &\quad + H_1(\varepsilon_{x,[0,N-L_t]}^d) \hat{\alpha}(t) - \hat{\sigma}^x(t - L_t | t)\|_{P_2}^2 \\ &\quad + 2 \sum_{k \in \mathbb{I}_{[t-L_t,t-1]} \cap \Omega} \eta^{t-k-1} \|h(\tilde{x}(k), u(k)) \\ &\quad \quad - h(\tilde{x}'(k), u(k))\|_R^2 \\ &\quad + 2\|H_1(\varepsilon_{x,[L_t-1,N-1]}^d) \hat{\alpha}(t) + \hat{\sigma}^x(t | t)\|_{P_1}^2.\end{aligned}\quad (\text{A.5})$$

In order to obtain an expression for $h(\tilde{x}'(k), u(k))$, from the second block row of (9b), we establish

$$\begin{aligned}H_{L_t}^{\tilde{\Omega}_t}(y_{[0,N-2]}^d) \hat{\alpha}(t) + H_{L_t}^{\tilde{\Omega}_t}(\varepsilon_{y,[0,N-2]}^d) \hat{\alpha}(t) \\ = \tilde{y}_{[t-L_t,t-1]} \cap \Omega - \hat{\sigma}_{[-L_t,-1]}^y(t).\end{aligned}\quad (\text{A.6})$$

Since for $k \in \mathbb{I}_{[t-L_t,t-1]} \cap \Omega$, it holds that $h(\tilde{x}'(k), u(k)) = H_1(y_{[k-(t-L_t),k-t+N]}^d) \hat{\alpha}(t)$, from (A.6) it follows that

$$\begin{aligned}\sum_{k \in \mathbb{I}_{[t-L_t,t-1]} \cap \Omega} h(\tilde{x}'(k), u(k)) \\ = \sum_{k \in \mathbb{I}_{[t-L_t,t-1]} \cap \Omega} (\tilde{y}(k) - \hat{\sigma}^y(k | t) \\ - H_1(\varepsilon_{y,[k-(t-L_t),k-t+N]}^d) \hat{\alpha}(t)).\end{aligned}$$

Using this result, adding zero to the first term on the right hand side of (A.5), and repeatedly using the fact that $\|a + b\|_P^2 \leq 2\|a\|_P^2 + 2\|b\|_P^2$ for $P \succ 0$, we can rewrite (A.5) as

$$\begin{aligned}\|x(t) - \hat{x}(t)\|_{P_1}^2 &\leq 8\lambda_{\max}(P_2, P_1) \|x(t - L_t) - \hat{x}(t - L_t)\|_{P_2}^2 \eta^{L_t} \\ &\quad + \sum_{k \in \mathbb{I}_{[t-L_t,t-1]} \cap \Omega} \left(8\|v(k)\|_R^2 \eta^{t-k-1} + 4\|\hat{\sigma}^y(k | t)\|_R^2 \eta^{t-k-1} \right. \\ &\quad \quad \left. + 8\|H_1(\varepsilon_{y,[k-(t-L_t),k-t+N]}^d) \hat{\alpha}(t)\|_R^2 \eta^{t-k-1} \right) \\ &\quad + 8\lambda_{\max}(P_2, P_1) \|\hat{x}(t - L_t) - \hat{x}(t - L_t | t)\|_{P_2}^2 \eta^{L_t} \\ &\quad + 8\lambda_{\max}(P_2, P_1) \|H_1(\varepsilon_{x,[0,N-L_t]}^d) \hat{\alpha}(t)\|_{P_2}^2 \eta^{L_t} \\ &\quad + 8\lambda_{\max}(P_2, P_1) \|\hat{\sigma}^x(t - L_t | t)\|_{P_2}^2 \eta^{L_t} \\ &\quad + 4\|H_1(\varepsilon_{x,[L_t-1,N-1]}^d) \hat{\alpha}(t)\|_{P_1}^2 + 4\|\hat{\sigma}^x(t | t)\|_{P_1}^2.\end{aligned}\quad (\text{A.7})$$

Part III: Combine the exponential i-OSS property with solutions of the MHE optimization problem

The established bound in (A.7) still depends on terms that come from the optimal solution to the MHE optimization problem (9). In the following, we exploit optimality properties to bound the terms of the optimal solution with terms from the solution of the candidate trajectory.

Thus, we now bound (A.7) by considering the cost of the optimal trajectory, which is given by

$$\begin{aligned} J^* = & 2\|\hat{x}(t - L_t|t) - \hat{x}(t - L_t)\|_{P_2}^2 \eta^{L_t} \\ & + \sum_{k \in \mathbb{I}_{[t-L_t, t-1]} \cap \Omega} \eta^{t-k-1} \|\hat{\sigma}^y(k|t)\|_R^2 \\ & + c_{\sigma^x} \|\hat{\sigma}_{[-L_t, 0]}^x(t)\|^2 + c_\alpha((\bar{\varepsilon}_x^d)^2 + (\bar{\varepsilon}_y^d)^2) \|\hat{\alpha}(t)\|^2. \end{aligned}$$

The first two terms of (A.7) do not need to be bounded, since they already consider the real unknown system state and measurement noise. Next, we consider the following terms

$$\begin{aligned} & 8\lambda_{\max}(P_2, P_1) \|\hat{x}(t - L_t) - \hat{x}(t - L_t|t)\|_{P_2}^2 \\ & + 4 \sum_{k \in \mathbb{I}_{[t-L_t, t-1]} \cap \Omega} \|\hat{\sigma}^y(k|t)\|_R^2 \eta^{t-k-1}. \end{aligned} \quad (\text{A.8})$$

These terms appear in the same way in the cost of the optimal trajectory with an additional factor 4 (and $\lambda_{\max}(P_2, P_1)$ for the prior weighting). Next, we consider

$$\begin{aligned} & \sum_{k \in \mathbb{I}_{[t-L_t, t-1]} \cap \Omega} 8\|H_1(\varepsilon_{y, [k-(t-L_t), k-t+N]}^d) \hat{\alpha}(t)\|_R^2 \eta^{t-k-1} \\ & \leq 8 \frac{\eta - \eta^L}{1 - \eta} (\bar{\varepsilon}_y^d)^2 p N \lambda_{\max}(R) \|\hat{\alpha}(t)\|^2. \end{aligned} \quad (\text{A.9})$$

Then, we consider

$$\begin{aligned} & 8\lambda_{\max}(P_2, P_1) \|H_1(\varepsilon_{x, [0, N-L_t]}^d) \hat{\alpha}(t)\|_{P_2}^2 \eta^{L_t} \\ & + 4\|H_1(\varepsilon_{x, [L_t-1, N-1]}^d) \hat{\alpha}(t)\|_{P_1}^2 \\ & \leq (8\lambda_{\max}(P_2, P_1) \lambda_{\max}(P_2) + 4\lambda_{\max}(P_1)) (\bar{\varepsilon}_x^d)^2 n N \|\hat{\alpha}(t)\|^2. \end{aligned}$$

Finally, since c_α and c_{σ^x} satisfy (14) and (15), respectively, we can bound the RHS of (A.7) as follows

$$\begin{aligned} & \|x(t) - \hat{x}(t)\|_{P_1}^2 \\ & \leq 8\lambda_{\max}(P_2, P_1) \|x(t - L_t) - \hat{x}(t - L_t)\|_{P_2}^2 \eta^{L_t} \\ & + \sum_{k \in \mathbb{I}_{[t-L_t, t-1]} \cap \Omega} (8\|v(k)\|_R^2 \eta^{t-k-1}) + 4\lambda_{\max}(P_2, P_1) J^* \end{aligned} \quad (\text{A.10})$$

Then, we use

$$J^* \leq J_{\text{cand}} \quad (\text{A.11})$$

where J_{cand} is the cost of the candidate trajectory defined by (Wolff et al., 2024b, Eq. (22) - (27)). Inequality (A.11) holds due to optimality. Considering (A.11) in (A.10) results in

$$\begin{aligned} & \|x(t) - \hat{x}(t)\|_{P_1}^2 \\ & \leq 8\lambda_{\max}(P_2, P_1) \|x(t - L_t) - \hat{x}(t - L_t)\|_{P_2}^2 \eta^{L_t} \\ & + \sum_{k \in \mathbb{I}_{[t-L_t, t-1]} \cap \Omega} (8\|v(k)\|_R^2 \eta^{t-k-1}) \\ & + 4\lambda_{\max}(P_2, P_1) (2\|x(t - L_t) - \hat{x}(t - L_t)\|_{P_2}^2 \eta^{L_t} \\ & + \sum_{k \in \mathbb{I}_{[t-L_t, t-1]} \cap \Omega} \eta^{t-k-1} \|v(k)\|_R^2 \\ & + c_{\sigma^x} \|\sigma_{[-L_t, 0]}^x(t)\|^2 + c_\alpha((\bar{\varepsilon}_x^d)^2 + (\bar{\varepsilon}_y^d)^2) \|\alpha(t)\|^2). \end{aligned} \quad (\text{A.12})$$

We simplify (A.12) and obtain

$$\begin{aligned} & \|x(t) - \hat{x}(t)\|_{P_1}^2 \\ & \leq 16\lambda_{\max}(P_2, P_1) \|x(t - L_t) - \hat{x}(t - L_t)\|_{P_2}^2 \eta^{L_t} \\ & + (8 + 4\lambda_{\max}(P_2, P_1)) \sum_{k \in \mathbb{I}_{[t-L_t, t-1]} \cap \Omega} \|v(k)\|_R^2 \eta^{t-k-1} \\ & + 4\lambda_{\max}(P_2, P_1) c_{\sigma^x} \|\sigma_{[-L_t, 0]}^x(t)\|^2 \\ & + 4\lambda_{\max}(P_2, P_1) c_\alpha((\bar{\varepsilon}_x^d)^2 + (\bar{\varepsilon}_y^d)^2) \|\alpha(t)\|^2. \end{aligned} \quad (\text{A.13})$$

We note that $u(t)$ and $x(t)$ evolve in a compact set, compare Assumption 3. Hence, there exist a u_{\max} and an x_{\max} so that $\|u(t)\| \leq u_{\max}$ and $\|x(t)\| \leq x_{\max} \quad \forall t \in \mathbb{I}_{\geq 0}$. Thus, we can bound $\alpha(t)$ as defined in (Wolff et al., 2024b, Eq. (23)) by

$$\|\alpha(t)\| \leq H_{ux} \sqrt{Lu_{\max} + x_{\max}} =: \alpha_{\max} \quad (\text{A.14})$$

with

$$H_{ux} = \max_{0 \leq t \leq L} \left\| \begin{pmatrix} H_{L_t}(u_{[0, N-1]}^d) \\ H_1(x_{[0, N-L_t-1]}^d) \end{pmatrix} \right\| \quad (\text{A.15})$$

and σ^x as defined in (Wolff et al., 2024b, Eq. (25)) by

$$\begin{aligned} \|\sigma_{[-L_t, 0]}^x(t)\|^2 & \leq n(L_t + 1) \|H_{L_t+1}(\varepsilon_{x, [0, N-1]}^d)\|_{\infty}^2 \|\alpha_{\max}\|^2 \\ & \leq n(L + 1) N^2 (\bar{\varepsilon}_x^d)^2 \alpha_{\max}^2 =: \sigma_{\max}^x. \end{aligned} \quad (\text{A.16})$$

We define

$$\begin{aligned} c(\bar{\varepsilon}^d) & := 4\lambda_{\max}(P_2, P_1) c_{\sigma^x} \sigma_{\max}^x \\ & + 4\lambda_{\max}(P_2, P_1) c_\alpha((\bar{\varepsilon}_x^d)^2 + (\bar{\varepsilon}_y^d)^2) \alpha_{\max}^2. \end{aligned} \quad (\text{A.17})$$

This results in

$$\begin{aligned} & \|x(t) - \hat{x}(t)\|_{P_1}^2 \\ & \leq 16\lambda_{\max}(P_2, P_1) \|x(t - L_t) - \hat{x}(t - L_t)\|_{P_2}^2 \eta^{L_t} \\ & + (8 + 4\lambda_{\max}(P_2, P_1)) \sum_{k \in \mathbb{I}_{[t-L_t, t-1]} \cap \Omega} \|v(k)\|_R^2 \eta^{t-k-1} \\ & + c(\bar{\varepsilon}^d). \end{aligned}$$

Now, we set $L_{\min} \in \mathbb{I}$ such that

$$\rho^{L_{\min}} := 16\lambda_{\max}(P_2, P_1)^2 \eta^{L_{\min}} < 1 \quad (\text{A.18})$$

is satisfied, choose $L \geq L_{\min}$, consider $t \in \mathbb{I}_{\geq L}$ and obtain

$$\begin{aligned} & \|x(t) - \hat{x}(t)\|_{P_1}^2 \leq \rho^L \|x(t - L) - \hat{x}(t - L)\|_{P_1}^2 \\ & + \sum_{k \in \mathbb{I}_{[t-L, t-1]} \cap \Omega} (8 + 4\lambda_{\max}(P_2, P_1)) \|v(k)\|_R^2 \eta^{t-k-1} + c(\bar{\varepsilon}^d). \end{aligned}$$

Applying this contraction recursively and following similar steps as in the proof of (Schiller et al., 2023, Cor. 1), we get

$$\begin{aligned} & \|x(t) - \hat{x}(t)\|_{P_1} \leq \tilde{\rho}^t \sqrt{\lambda_{\max}(P_2, P_1)} \|x(0) - \hat{x}(0)\|_{P_2} \\ & + \sqrt{8 + 4\lambda_{\max}(P_2, P_1)} \sum_{k \in \mathbb{I}_{[0, t-1]} \cap \Omega} \|v(k)\|_R \tilde{\rho}^{t-k-1} + \tilde{\gamma}(\bar{\varepsilon}^d) \end{aligned}$$

with $\gamma(\bar{\varepsilon}) := (1/(1 - \rho))c(\bar{\varepsilon})$, $\tilde{\rho} := \sqrt{\rho}$, and $\tilde{\gamma} := \sqrt{\gamma} \in \mathcal{K}$ resulting in the desired expression. ■